

Dynamics of Relativistic Flows

C. Chicone

Department of Mathematics
University of Missouri-Columbia
Columbia, Missouri 65211, USA

B. Mashhoon*

Department of Physics and Astronomy
University of Missouri-Columbia
Columbia, Missouri 65211, USA

B. Punsly

4014 Emerald Street, No. 116
Torrance, California 90503, USA

June 27, 2018

Abstract

Dynamics of relativistic outflows along the rotation axis of a Kerr black hole is investigated using a simple model that takes into account the relativistic tidal force of the central source as well as the Lorentz force due to the large-scale electromagnetic field which is assumed to be present in the ambient medium. The evolution of the speed of the flow relative to the ambient medium is studied. In the force-free case, the resulting equation of motion predicts rapid deceleration of the initial flow and an asymptotic relative speed with a Lorentz factor of $\sqrt{2}$. In the presence of the Lorentz force, the long-term relative speed of the clump tends to the ambient electrical drift speed.

Key words: relativity; black holes; jets

1 Introduction

A significant feature associated with quasars and active galactic nuclei is the existence of relativistic outflows known as “jets.” The jets frequently come in pairs that originate from a central “engine” that is conjectured to be a massive rotating black hole surrounded by an accretion disk. Rather similar phenomena

*Corresponding author. E-mail: mashhoonb@missouri.edu (B. Mashhoon).

are also observed in most of the X-ray binary systems in our galaxy; therefore, these are usually called “microquasars.” It is thought that the jets are emitted along the rotation axis of the Kerr black hole. The double-jet structure is consistent with the symmetry of a Kerr source under reflection about its equatorial plane as illustrated in Figure 1. The observational aspects of the motion of astrophysical jets are discussed in [1, 2, 3, 4].

The purpose of this paper is to discuss a relativistic tidal effect that can be used to predict the speeds of astrophysical jets relative to their ambient media. The theory of the formation and propagation of jets per se is beyond the scope of this paper. We will consider a Kerr black hole with plasma outflow along its rotation axis and study the dynamics of a clump in the flow *after it has emerged from its source environment*. To explore the transient role of the novel relativistic tidal effect near the source, we assume that large-scale electromagnetic fields are dynamically important. We thus ignore the complicated plasma processes that actually determine the electrical drift velocity of the ambient medium. Our approach may be contrasted with the purely hydrodynamic models of relativistic outflows: all force-free as well as MHD wind models assume at the outset that the plasma flows at the drift velocity. It is important to emphasize the idealized nature of the model employed here; our purpose is simply to illustrate the regime in which previously ignored relativistic tidal forces are significant for the dynamics of relativistic outflows.

The mechanism for clump formation and the possible values of the clump’s initial speed as well as other characteristics are beyond the scope of our paper. Once emitted, the motion of the clump relative to the ambient medium is subject to the ubiquitous tidal forces of the central source together with the Lorentz force due to the large-scale electromagnetic field that is assumed to be present in the ambient medium. In addition to various other simplifying assumptions throughout this work, all radiative as well as nonlinear plasma effects [5, 6] are also neglected here.

With respect to a background Fermi frame that is fixed on the ambient medium with coordinates (T, \mathbf{X}) such that $\mathbf{X} = (X, Y, Z)$ and the Z -axis represents the axis of rotation of the black hole, the equation of motion of a plasma clump along the rotation axis relative to the ambient medium is given by a “Newtonian” equation of motion, involving the superposition of external accelerations, of the form

$$\frac{d^2 Z}{dT^2} = A_T + A_L, \quad (1)$$

where A_T is the relativistic tidal acceleration due to the central rotating mass and A_L is the Lorentz acceleration due to the electromagnetic field of the ambient medium. The nature of these accelerations are discussed in turn in Sections 2, 3 and 4. The main dynamical features of the resulting equation of motion are described in Section 5. Section 6 contains a brief discussion of our results. We employ units such that $c = 1$.

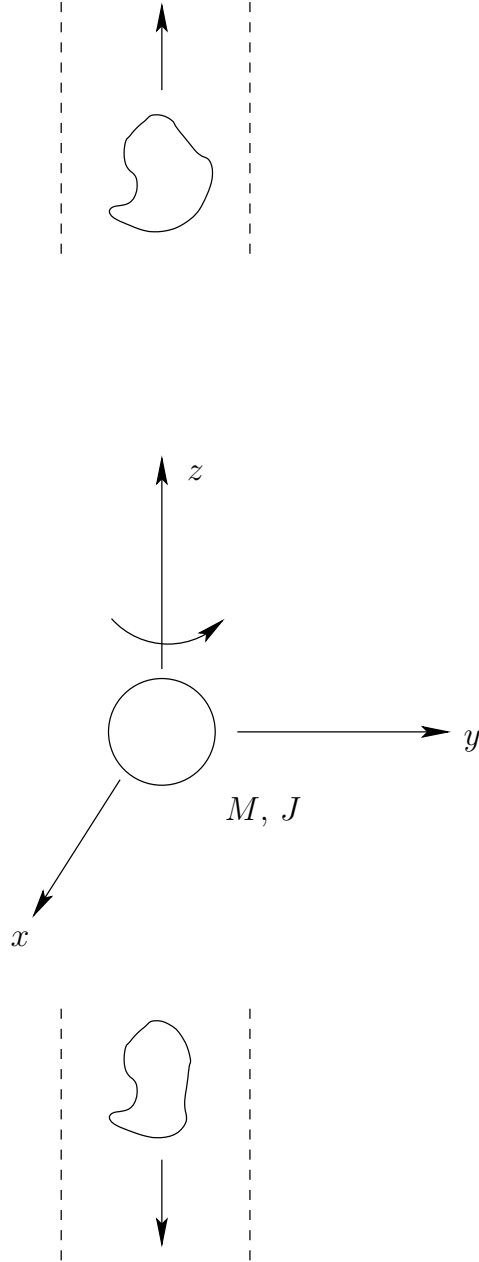


Figure 1: Schematic diagram representing jet clumps moving relative to the ambient medium along the rotation axis of a central black hole.

2 The Generalized Jacobi Equation

Imagine a background global inertial system with coordinates (T, \mathbf{X}) and two neighboring test particles in free fall in a Newtonian gravitational potential $\Phi(\mathbf{X})$. Let $\mathbf{X}_1(T)$ and $\mathbf{X}_2(T)$ denote the paths of the two particles. Neglecting the gravitational attraction between the test particles, their relative position $\mathbf{X}(T) = \mathbf{X}_1(T) - \mathbf{X}_2(T)$ is determined by the tidal equation

$$\frac{d^2 X^i}{dT^2} + K_{ij}(T)X^j = 0, \quad (2)$$

where $K = (K_{ij})$ is a symmetric matrix given by

$$K_{ij} = \frac{\partial^2 \Phi}{\partial X^i \partial X^j} \quad (3)$$

evaluated along the orbit of one of the particles designated as the reference trajectory. Note that $\text{tr}(K) = \nabla^2 \Phi = 4\pi G \rho_N$, where ρ_N is the Newtonian mass density of the source. If the motion occurs exterior to the source, then the matrix K given by (3) is trace-free and harmonic. The tidal acceleration in (2) has been evaluated to linear order in the separation of the particles.

In the theoretical framework of general relativity, the free neighboring test particles follow timelike geodesics of the spacetime manifold. Their relative motion is described by the geodesic deviation equation. This equation may be expressed in terms of a Fermi normal coordinate system that is constructed along the reference geodesic. A Fermi frame is an almost inertial coordinate system in a finite cylindrical region along the worldline of the reference geodesic [7]. We now let (T, \mathbf{X}) refer to the Fermi coordinates in such a system, where the spatial origin $\mathbf{X} = 0$ is occupied by the fiducial test particle. Then, the Jacobi equation (2) describes the relative motion of the other test particle in Fermi coordinates and

$$K_{ij} = {}^F R_{0i0j}, \quad (4)$$

provided that the speed of relative motion is negligibly small compared to $c = 1$. Here

$${}^F R_{\alpha\beta\gamma\delta} = R_{\mu\nu\rho\sigma} \lambda_{(\alpha)}^\mu \lambda_{(\beta)}^\nu \lambda_{(\gamma)}^\rho \lambda_{(\delta)}^\sigma, \quad (5)$$

so that the Riemann tensor in the Fermi frame evaluated along the reference trajectory $(T, \mathbf{0})$ is in effect the Riemann tensor projected onto the nonrotating orthonormal tetrad $\lambda_{(\alpha)}^\mu$ that is carried along the fiducial geodesic and upon which the Fermi system is constructed. Specifically, the temporal axis of the fiducial observer $\lambda_{(0)}^\mu = dx^\mu/d\tau$ is the vector tangent to its worldline, τ is its proper time and $\lambda_{(i)}^\mu, i = 1, 2, 3$, are its spatial axes. One can show explicitly that in the Newtonian approximation of general relativity (4) reduces to (3), so that the formal analogy developed here has a deep physical basis.

The deviation between geodesics is taken into account only to linear order in the Jacobi equation; in fact, higher-order terms can be neglected so long as the deviation is very small compared to the radius of curvature of spacetime \mathcal{R} .

On the other hand, in certain circumstances, the relative speed of neighboring geodesics may not be small compared to unity. The corresponding generalization of the Jacobi equation is given by

$$\begin{aligned} \frac{d^2 X^i}{dT^2} + {}^F R_{0i0j} X^j + 2 {}^F R_{ikj0} V^k X^j \\ + (2 {}^F R_{0kj0} V^i V^k + \frac{2}{3} {}^F R_{ikj\ell} V^k V^i + \frac{2}{3} {}^F R_{0kj\ell} V^i V^k V^\ell) X^j = 0. \end{aligned} \quad (6)$$

This generalized Jacobi equation has been discussed in detail in [8]. If we limit our attention to motion along a fixed direction in space, say along the Z -direction that characterizes the rotation axis of a Kerr system in the Fermi frame, then (6) reduces to

$$\frac{dV}{dT} + \kappa(1 - 2V^2)Z = 0, \quad (7)$$

where $V = dZ/dT$ and $\kappa = {}^F R_{0303}$. This equation has an interesting feature that was first pointed out in [8]: Special solutions of (7) exist that correspond to uniform rectilinear motion with limiting velocities of $V_T = \pm(2)^{-\frac{1}{2}}$. For $\kappa < 0$, these correspond to attractors if

$$\int_{T_0}^{\infty} \kappa(T)(T + C_0)dT = -\infty \quad (8)$$

for an arbitrary real number C_0 and an arbitrary initial time T_0 [8].

It is useful to consider the application of (7) to motion along the rotation axis of a Kerr source. The main results are expected to hold qualitatively for any central rotating and axisymmetric configuration such as, for instance, the Kerr spacetime endowed with an infinite set of higher moments [9]. The motion of free test particles along the symmetry axis of an exterior Kerr spacetime representing the stationary gravitational field of a source of mass M and angular momentum Ma is given by

$$\left(\frac{dr}{d\tau}\right)^2 = \gamma^2 - 1 + \frac{2GMr}{r^2 + a^2} \quad (9)$$

in Boyer-Lindquist coordinates. Here $\gamma > 0$ is an integration constant; in fact, in the $\gamma \geq 1$ case it has the interpretation of the particle's Lorentz factor at infinity ($r \rightarrow \infty$). We take the reference geodesic to represent the motion of the ambient medium with $dr/d\tau > 0$ along the Z -axis in the exterior Kerr spacetime and we construct a Fermi coordinate system (T, X, Y, Z) in the neighborhood of this geodesic such that as the reference geodesic is approached, $(T, \mathbf{X}) \rightarrow (\tau, \mathbf{0})$. Evaluating the Riemann curvature tensor in this frame, we find that $\kappa \rightarrow k$ is given by

$$k = -2 \frac{GMr(r^2 - 3a^2)}{(r^2 + a^2)^3}. \quad (10)$$

That (10) is explicitly independent of γ is a consequence of the fact that Kerr spacetime is of type D in the Petrov classification and hence the axis of rotation

provides two special tidal directions for ingoing and outgoing trajectories [10, 11]. Moreover, $a = 0$ corresponds to radial motion in the exterior Schwarzschild spacetime. For a Kerr black hole $0 < a \leq GM$, where $a = GM$ corresponds to an extreme Kerr black hole. To emphasize that our treatment involves motion along the rotation axis of a Kerr system, it is useful to introduce Cartesian coordinates (x, y, z) defined in terms of Boyer-Lindquist coordinates (r, θ, φ) as usual: $x = r \sin \theta \cos \varphi$, $y = r \sin \theta \sin \varphi$ and $z = r \cos \theta$. In Section 5, we will employ this z -coordinate along the Kerr rotation axis that in the Fermi system becomes the Z -axis. Moreover, we will assume that the reference particle at $Z = 0$ is such that $\gamma = 1$ and $r > \sqrt{3}a$ along its geodesic path. The $\gamma = 1$ condition implies that the reference particle moves away from the black hole forever, coming to rest at infinity. The collection of such particles provides an ambient medium with respect to which the motion of the jet clump can be described. That is, this ambient medium provides a dynamical way of characterizing the rest frame of the black hole.

Imagine two neighboring test particles at r and $r + \delta r$ along the rotation axis of a central source. Far away from the source, the Newtonian gravitational acceleration of the reference particle at r is $-GM/r^2$ and for the other particle at $r + \delta r$ is $-GM/(r + \delta r)^2$. The relative or tidal acceleration is then given by $2GM\delta r/r^3$, which by (10) is $-k\delta r$ for $r \gg GM$ and $r \gg a$. Therefore, (7) and (10) reduce to the familiar Newtonian result once the relativistic tidal acceleration proportional to $V^2 \ll 1$ is neglected.

The speed of a clump can be measured by observing the displacement of the clump in the flow relative to the ambient medium [1, 2, 3, 4]. Therefore, consider a clump along the axis of rotation moving rapidly past the reference particle belonging to the ambient medium. The equation of relative motion is given by (1) with

$$A_T = -k(1 - 2V^2)Z, \quad (11)$$

where k is determined via equations (9) and (10). Under our assumption we have that $r^2 > 3a^2$, and thus $k < 0$. Also, we have assumed that $\gamma = 1$ in (9) for the ambient medium surrounding the black hole; therefore, condition (8) is satisfied, the two special solutions of (11) are indeed attractors and the clump speed (predicted by our model) tends to ≈ 0.7 over time [8]. In [8] a similar assertion was also made for $\gamma < 1$, which turns out to be erroneous in general; in any case, it is not relevant for a black hole source with $a \leq GM$. The qualitative dependence of the solution of the generalized Jacobi equation upon $\gamma \geq 1$ is depicted in Figure 2; in constructing this figure, we consider equation (11) simply as a nonlinear differential equation and ignore its possible physical limitations.

It is important to recognize two salient features of equation (11) for the force-free motion of an ultrarelativistic clump relative to the ambient medium with $\gamma = 1$. First, the initial deceleration of the clump can be quite significant *within the range of validity* of the generalized Jacobi equation (11). For instance, Figure 3 depicts the deceleration of clumps with initial Lorentz factors of $\Gamma_0 = 20, 10$ and 5 , where we have introduced the Lorentz factor of the clump $\Gamma =$

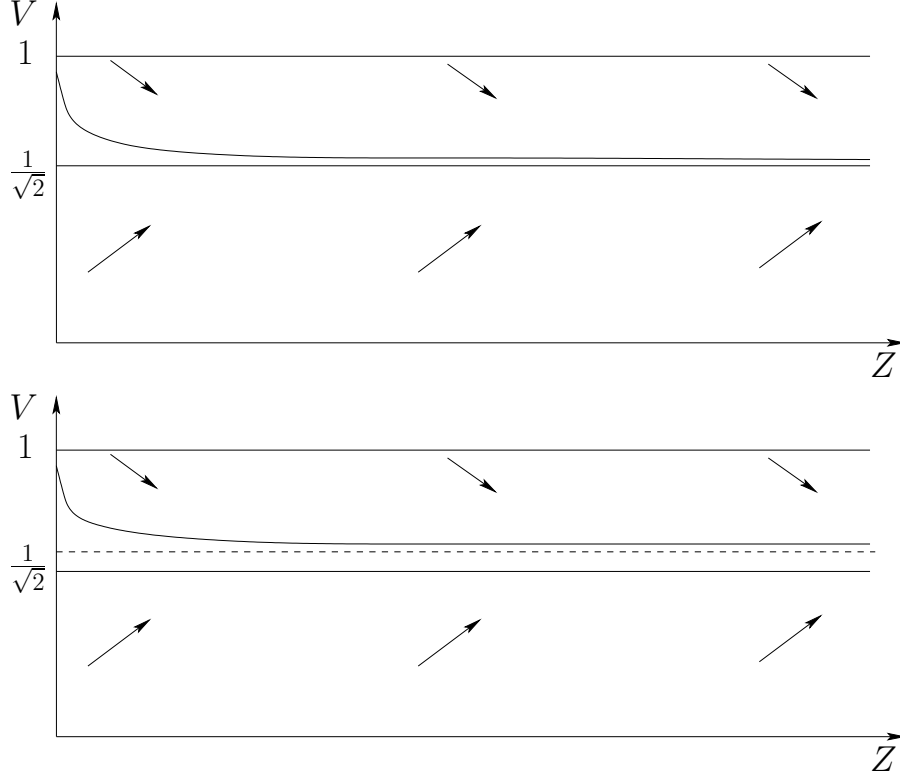


Figure 2: Schematic representation of direction fields and trajectories for the force-free case given by the generalized Jacobi equation. Equation (11) is integrated with the initial conditions that at $T = 0$, $r = r_0 > \sqrt{3}a$, $Z = 0$ and $V = V_0 > 0$; thus, initially $dV/dZ = 0$ as well. The top panel depicts a trajectory for $\gamma = 1$. In this case the velocity is asymptotic to $1/\sqrt{2}$. The bottom panel depicts a trajectory for $\gamma > 1$. In this case, the trajectory is asymptotic to some constant velocity, depicted by the dashed line, that is closer to $1/\sqrt{2}$ than the initial velocity. The limiting velocity can be calculated, in principle, from the integration of the generalized Jacobi equation $V dV/dZ = -k(1 - 2V^2)Z$, namely, $1 - 2V^2 = (1 - 2V_0^2) \exp(4 \int_0^Z k(T(Z'))Z' dZ')$. For $\gamma = 1$, the integral as $Z \rightarrow \infty$ is $-\infty$ in agreement with (8) and hence the limiting velocity is given by $V = 1/\sqrt{2}$.

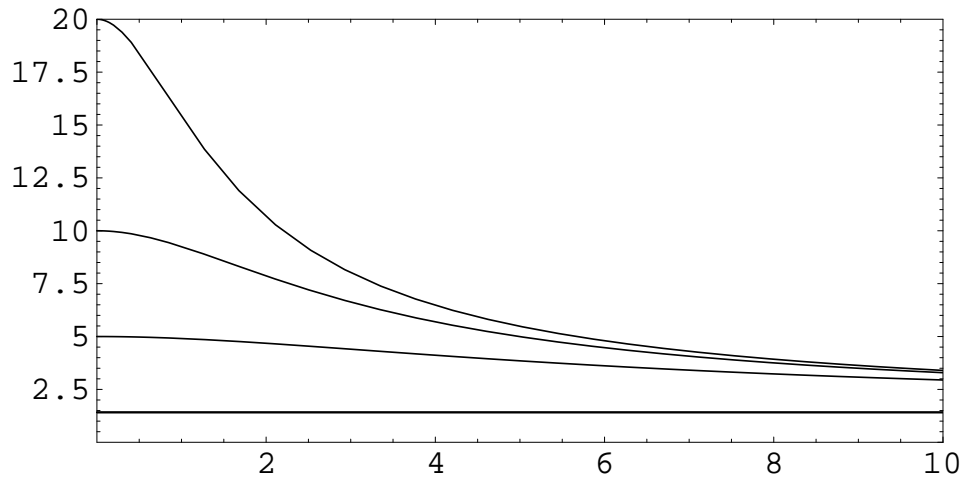


Figure 3: Plot of the Lorentz factor $\Gamma = (1 - V^2)^{-1/2}$ versus $T/(GM)$ based on the integration of equation (11) with initial data $r_0/(GM) = 10$, $Z(0) = 0$, $V(0) = 2\sqrt{6}/5 \approx 0.980$, $3\sqrt{11}/10 \approx 0.991$ and $\sqrt{399}/20 \approx 0.999$ corresponding to $\Gamma_0 = 5$, 10 and 20, respectively. Here we assume that $a/(GM) = 1$ and $\gamma = 1$. At $T/(GM) = 10$ the corresponding Lorentz factors are $\Gamma \approx 2.945$, 3.291 and 3.398, respectively. For the sake of comparison, the horizontal line indicates the Lorentz factor $\sqrt{2}$ corresponding to the terminal speed. Further away from the central source, the tidal forces decrease and hence the initial deceleration is correspondingly weaker. For instance, with $r_0/(GM) = 100$, the clump decelerates from $\Gamma_0 = 5$ to $\Gamma = 3$ over a time interval given approximately by $T/(GM) = 300$.

$(1 - V^2)^{-1/2}$, and Γ_0 corresponds to the initial clump speed V_0 at $r = r_0$ and $T = Z = 0$. Launched from $r_0 = 10 GM$, the clumps decelerate to $\Gamma \approx 3$ in about $T = 10 GM \approx 5 \times 10^{-5} (M/M_\odot)$ sec. Although the distance of such a clump relative to the reference particle increases rapidly and soon the validity of the generalized Jacobi equation breaks down, the subsequent motion can be measured with the same model equation relative to the motion of another suitable reference particle in the ambient medium. This observation uses the second remarkable feature of equation(11): it does not explicitly depend on the choice of the reference particle in the ambient medium with $\gamma = 1$. To illustrate this point, imagine a sequence of n reference particles at r_i , $i = 1, 2, \dots, n$, all with $\gamma = 1$ along the rotation axis of the central source such that $r_1 < r_2 < \dots < r_i < r_{i+1} < \dots < r_n$. We can set up distinct Fermi frames along the worldline of each of these reference particles such that within each interval $[r_i, r_{i+1}]$ the generalized Jacobi equation is valid in the Fermi frame based on r_i . Once the clump reaches r_{i+1} , we can switch to the new Fermi frame based on r_{i+1} . So long as the initial speed of the clump relative to r_{i+1} is above $1/\sqrt{2}$, the model predicts that the clump continues to decelerate toward the terminal speed. In this sense, the speed of the clump *relative to the ambient medium* approaches the terminal speed over time.

In the absence of any nongravitational forces, equations (1) and (11) express the geodesic equation for the center of mass of the clump in Fermi coordinates. Once the electromagnetic forces are included, the general equation of motion takes the form

$$\rho'_m \left(\frac{d^2 x^\mu}{ds^2} + \Gamma_{\nu\rho}^\mu \frac{dx^\nu}{ds} \frac{dx^\rho}{ds} \right) = F^\mu{}_\sigma j^\sigma, \quad (12)$$

where ρ'_m is the invariant mass density of the clump, $F_{\mu\nu}$ is the Faraday tensor of the exterior electromagnetic field in the ambient medium and j^μ is the charge current of the clump. Expressed in the Fermi coordinate system (T, \mathbf{X}) , equation (12) reduces to equation (1), where A_L is due to the Lorentz force. In evaluating the Lorentz acceleration A_L in the following section, we employ the physically reasonable approximation that the effects of spacetime curvature can be neglected for the sake of simplicity; thus, we treat the Fermi frame established along the reference geodesic as an inertial frame of reference in Section 3.

It is conceivable that the electromagnetic field configuration is such that $F^\mu{}_\sigma j^\sigma = 0$ in equation (12) and hence the motion of the clump is force-free (see, for example, [12]). This may be the case, for instance, beyond the launching point of the flow, a few gravitational radii from the central source. In the force-free case, the detailed analysis of [8] is applicable in the sense explained above and the clump speed tends to $1/\sqrt{2} \approx 0.7$, corresponding to a Lorentz factor of $\sqrt{2} \approx 1.4$. Our results may be of interest in connection with Galactic superluminal sources [3, 4]; in fact, as already pointed out in [8], some of these superluminal jets have speeds that may be near $1/\sqrt{2} \approx 0.7$. In the rest of this paper, we investigate clump motion that is *not* force-free.

3 Lorentz Acceleration

Imagine a definite clump of plasma with constant mass m moving with respect to the ambient medium with velocity $\mathbf{V} = V\hat{\mathbf{n}}$, where $\hat{\mathbf{n}}$ is a fixed direction in space that will be later identified with the rotation axis of the central gravitational source. The Lorentz force law for the motion of the clump can be written as

$$\frac{d}{dT} \left(\frac{mV}{\sqrt{1-V^2}} \right) = (\delta\mathcal{V})(\rho\mathbf{E} + \mathbf{J} \times \mathbf{B}) \cdot \hat{\mathbf{n}}, \quad (13)$$

where $\delta\mathcal{V}$, ρ and \mathbf{J} are, respectively, the volume, charge density and charge current of the clump with respect to the inertial frame (T, \mathbf{X}) . We assume that in the rest frame of the clump $m = \rho'_m \delta\mathcal{V}'$, where ρ'_m and $\delta\mathcal{V}'$ are the proper density and volume of the plasma clump, respectively, and are assumed to be constants throughout the motion under consideration here. Primed quantities refer to the rest frame of the clump. It follows from Lorentz contraction that (13) may be written as

$$\frac{d}{dT} \left(\frac{V}{\sqrt{1-V^2}} \right) = \frac{\sqrt{1-V^2}}{\rho'_m} (\rho\mathbf{E} + \mathbf{J} \times \mathbf{B}) \cdot \hat{\mathbf{n}}. \quad (14)$$

Moreover, we note that for one-dimensional motion

$$\frac{d}{dT} \left(\frac{V}{\sqrt{1-V^2}} \right) = (1-V^2)^{-3/2} \frac{dV}{dT}, \quad (15)$$

so that equation (14) reduces to

$$\frac{dV}{dT} = \frac{(1-V^2)^2}{\rho'_m} (\rho\mathbf{E} + \mathbf{J} \times \mathbf{B}) \cdot \hat{\mathbf{n}}. \quad (16)$$

We now turn to the electromagnetic aspects of (16) and assume that in the rest frame of the clump $\rho' = 0$ and that $\mathbf{J}' = \sigma\mathbf{E}'$ in accordance with Ohm's law. The electrical conductivity σ is a tensor in general; however, we take σ to be a scalar for the sake of simplicity. It follows from

$$\rho' = \Gamma(\rho - \mathbf{V} \cdot \mathbf{J}) \quad (17)$$

that $\rho = \mathbf{V} \cdot \mathbf{J} = VJ_{\parallel}$. This fact immediately implies that $J'_{\parallel} = \Gamma^{-1}J_{\parallel}$ using the transformation

$$J'_{\parallel} = \Gamma(J_{\parallel} - V\rho). \quad (18)$$

Thus, we have

$$\mathbf{J}'_{\perp} = \mathbf{J}_{\perp}, \quad J'_{\parallel} = \Gamma^{-1}J_{\parallel} \quad (19)$$

and at the same time

$$\mathbf{E}'_{\perp} = \Gamma(\mathbf{E} + \mathbf{V} \times \mathbf{B})_{\perp}, \quad E'_{\parallel} = E_{\parallel}. \quad (20)$$

It follows from (19), (20) and $\mathbf{J}' = \sigma\mathbf{E}'$ that

$$\mathbf{J} = \sigma\Gamma(\mathbf{E} + \mathbf{V} \times \mathbf{B}). \quad (21)$$

Thus $\rho = VJ_{\parallel} = \sigma\Gamma VE_{\parallel}$ and

$$(\rho\mathbf{E} + \mathbf{J} \times \mathbf{B}) \cdot \hat{\mathbf{n}} = \sigma\Gamma VE_{\parallel}^2 + \sigma\Gamma[(\mathbf{E} + \mathbf{J} \times \mathbf{B}) \times \mathbf{B}]_{\parallel}. \quad (22)$$

Using the identity

$$[(\mathbf{V} \times \mathbf{B}) \times \mathbf{B}]_{\parallel} = -V(B^2 - B_{\parallel}^2) = -VB_{\perp}^2, \quad (23)$$

we find that

$$(\rho\mathbf{E} + \mathbf{J} \times \mathbf{B}) \cdot \hat{\mathbf{n}} = \Gamma\sigma B^2(w - \frac{B_{\perp}^2 - E_{\parallel}^2}{B^2}V), \quad (24)$$

where

$$w = \frac{(\mathbf{E} \times \mathbf{B}) \cdot \hat{\mathbf{n}}}{B^2} \quad (25)$$

and

$$\mathbf{w}_D = \frac{\mathbf{E} \times \mathbf{B}}{B^2} \quad (26)$$

is the electrical drift velocity [13]. To proceed further, we need a model for the electromagnetic field configuration in the medium surrounding the black hole. This is considered in the next section.

4 A Simple Model

Let us now consider the magnetically dominated environment in which the clump is moving. In some models for such an environment [14] and in cylindrical coordinates (ρ, ϕ, z) with $\hat{\mathbf{n}} = \hat{\mathbf{z}}$, integrating Maxwell's equation $\nabla \cdot \mathbf{B} = 0$ implies that $B_z \sim \rho^{-2}$. If angular momentum is approximately conserved in the electromagnetic field, then $B_{\phi} \sim \rho^{-1}$. Thus, at large distances from the source, jets and collimated winds are often considered to have predominantly toroidal magnetic fields. Assuming that the plasma is efficient at maintaining a very small proper electric field through its conductive properties, this implies that \mathbf{E} is approximately radial in cylindrical coordinates [14]. It is clear from this brief description that in any reasonably realistic scenario the electromagnetic field configuration would be rather complicated. However, we seek a simple model situation that would render the resulting equation of motion amenable to mathematical analysis. Therefore, we assume that the average electric field is primarily radial, $\mathbf{E} = E\hat{\rho}$, and the average magnetic field is primarily azimuthal, $\mathbf{B} = B\hat{\phi}$, such that $E < B$. In view of the symmetry of the central source about its equatorial plane, in this paper we concentrate—for the sake of simplicity—only on the clump moving along the positive z -axis. It follows from (25) that the electrical drift speed is given by $w = E/B < 1$. Moreover, (24) takes the simple form $\Gamma(\sigma B^2)(w - V)$.

It turns out that in the rest frame of the clump $\mathbf{E}' = E'\hat{\rho}$ and $\mathbf{B}' = B'\hat{\phi}$, i.e. the fields have the same configuration as in the global inertial frame (T, \mathbf{X}) . Thus following the analysis in §2.10 of [14], the conductivity σ should be identified with σ_{\perp} as the current $\mathbf{J}' = \sigma_{\perp}\mathbf{E}'$ will be crossing the magnetic lines of

force in the local rest frame of the clump. On the other hand, for motion along the magnetic lines of force, the electrical conductivity σ_{\parallel} would have its usual value

$$\sigma_{\parallel} = \frac{n_e e^2 \tau_c}{\mu_e}, \quad (27)$$

where $-e$, n_e and μ_e are, respectively, the charge, number density and mass of the electron in the electron-proton plasma in the rest frame of the clump. Here the relaxation time $\tau_c = \nu_c^{-1}$ is the average time interval between electron collisions and hence ν_c is the average frequency of electron collisions per second. It follows from the discussion in §2.10 of [14] that in case of a tenuous plasma in a strong magnetic field such that $\nu_c^2 \ll \Omega_e^2$, we have

$$\frac{\sigma_{\perp}}{\sigma_{\parallel}} = \left(\frac{\nu_c}{\Omega_e} \right)^2, \quad (28)$$

where $\Omega_e = eB'/\mu_e$ is the cyclotron frequency for a free electron. Thus

$$\frac{\sigma_{\perp} B^2}{\rho'_m} = \left(\frac{\mu_e}{\mu_p} \right) \left(\frac{B}{B'} \right)^2 \nu_c, \quad (29)$$

where μ_p is the proton mass and $\rho'_m = n_p \mu_p + n_e \mu_e = n_e (\mu_p + \mu_e) \approx n_e \mu_p$, since $\rho' = 0$ implies that the density of protons in the clump is the same as that of electrons, $n_p = n_e$, and $\mu_p/\mu_e \approx 1836 \gg 1$. Moreover,

$$\mathbf{B}'_{\perp} = \Gamma(\mathbf{B} - \mathbf{V} \times \mathbf{E})_{\perp}, \quad (30)$$

which implies that

$$\frac{B'}{B} = \Gamma(1 - wV). \quad (31)$$

Combining these results with (16) reveals that the Lorentz acceleration is given by

$$A_L = \frac{dV}{dT} = \alpha \frac{(1 - V^2)^{5/2}}{(1 - wV)^2} (w - V), \quad (32)$$

where

$$\alpha = \left(\frac{\mu_e}{\mu_p} \right) \nu_c. \quad (33)$$

It is interesting to note that for copper at room temperature $\nu_c \sim 10^{14} \text{ sec}^{-1}$.

It follows from equations (32) and (33) that the Lorentz acceleration A_L vanishes if the clump speed is equal to the drift speed. Moreover, A_L is proportional to the collision frequency ν_c . This is due to the fact that only through collisions can an appropriate interior current be established that could lead to the acceleration of the clump along the flow direction.

It remains to provide an estimate of ν_c for the case of the electron-proton plasma under consideration here. This is a rather complicated problem and we therefore limit our investigation to the simpler case of collisions among the electrons while neglecting the motion of the protons. Thus we assume that τ_c

can be estimated using the “self-collision time” of electrons given by equation (5-26) of [13]

$$\tau_c^* = \frac{0.266 \mathcal{T}^{3/2}}{n_e \ln \Lambda} \text{sec}, \quad (34)$$

where \mathcal{T} is the absolute temperature and n_e is the number of electrons in the clump per cm^3 . Here Λ is essentially the ratio of two lengths: the Debye shielding distance over the characteristic impact parameter of electron collisions such that the deflection angle in the orbital plane is equal to $\pi/2$. One can use Table 5.1 of [13] to find the values of $\ln \Lambda$ in terms of \mathcal{T} and n_e . According to this table, for a fixed \mathcal{T} , $\ln \Lambda$ decreases very slowly but monotonically as n_e increases from $n_e = 1 \text{ cm}^{-3}$ to $n_e = 10^{24} \text{ cm}^{-3}$; for example, for $\mathcal{T} = 10^8 \text{ K}$, $\ln \Lambda$ monotonically decreases from 34.3 for $n_e = 1 \text{ cm}^{-3}$ to 6.69 for $n_e = 10^{24} \text{ cm}^{-3}$. Thus for $\mathcal{T} = 10^8 \text{ K}$ and $n_e = 10^6 \text{ cm}^{-3}$, we find $\ln \Lambda = 27.4$ and hence from (34) with $\nu_c \approx (\tau_c^*)^{-1}$ we obtain $\alpha \approx 0.56 \times 10^{-7} \text{ sec}^{-1}$. For fixed \mathcal{T} , α increases almost linearly with n_e such that for $n_e = 10^{15} \text{ cm}^{-3}$ in the case under discussion, we have $\alpha \approx 35 \text{ sec}^{-1}$ [13]. These considerations illustrate the fact that α could have a considerable range of values depending upon the electron temperature \mathcal{T} and density n_e .

5 Equation of Motion

The equation of motion of the clump is given by

$$\frac{d^2 Z}{dT^2} + k(T)(1 - 2V^2)Z = \alpha \frac{(1 - V^2)^{5/2}}{(1 - wV)^2} (w - V), \quad (35)$$

where $V = dZ/dT$, α is a characteristic of the plasma clump, w is a characteristic of the electromagnetic field of the ambient medium and k is essentially the curvature of the central source given by

$$k(T) = -\frac{2GMz(z^2 - 3a^2)}{(z^2 + a^2)^3}, \quad (36)$$

while $z(T)$ is determined using the geodesic equation for the background

$$\left(\frac{dz}{dT}\right)^2 = \gamma^2 - 1 + \frac{2GMz}{z^2 + a^2}. \quad (37)$$

The equation of motion (35) has been derived for the clump moving along the positive Z -axis. Recall that z in equations (36) and (37) is a substitute for the radial coordinate r . Therefore, let us note that equations (35)–(37) are invariant under the transformations $Z \rightarrow -Z$, $w \rightarrow -w$, $V \rightarrow -V$ and $z \rightarrow z$. Hence our results hold for the clump moving along the negative Z -direction as well.

It is useful to put equations (35)–(37) in dimensionless form. To this end, we assume that all lengths are measured in units of GM , which is one-half of

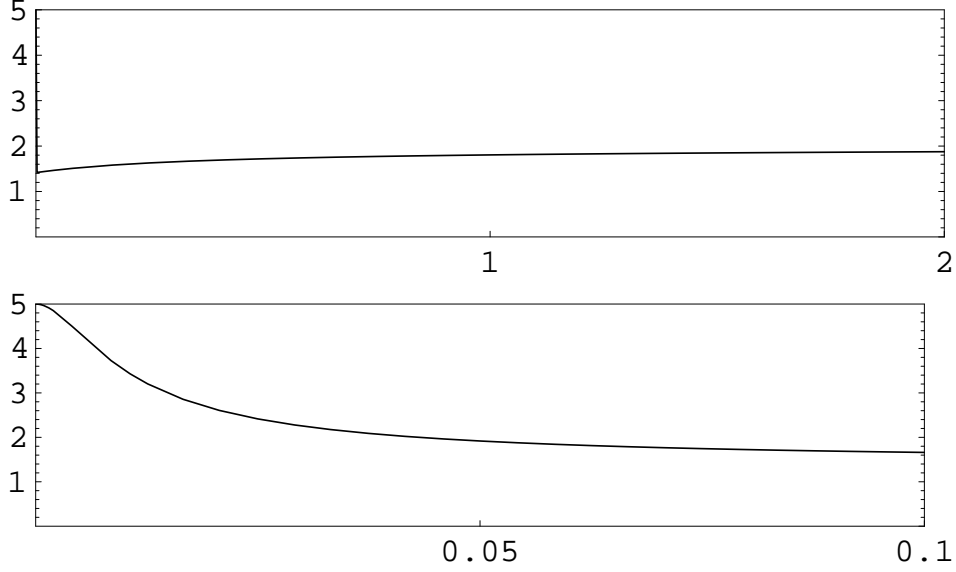


Figure 4: The top panel depicts the graph of the Lorentz factor Γ , given by $\Gamma(T) := (1 - V(T)^2)^{-1/2}$, versus time specified in hours. The bottom panel depicts the graph of Γ versus time specified in seconds. For these graphs, $\hat{a} = 1$, $\gamma = 1$, $\hat{\alpha} = 10^{-7}$, $w = \sqrt{3}/2 \approx .866$, $r_0/(GM) = z(0) = 100$, $Z(0) = 0$ and $V(0) = 2\sqrt{6}/5 \approx 0.980$. We assume that $M = 10M_\odot$, hence time is measured here in units of $GM = 10GM_\odot \approx 5 \times 10^{-5}$ sec.

the gravitational radius of the central source. Defining dimensionless quantities \hat{k} , $\hat{\alpha}$ and \hat{a} as

$$\hat{k} = (GM)^2 k, \quad \hat{\alpha} = GM\alpha, \quad \hat{a} = \frac{a}{GM} \quad (38)$$

we recover equations (35)–(37) in dimensionless form once we let $k \rightarrow \hat{k}$, $\alpha \rightarrow \hat{\alpha}$, $a \rightarrow \hat{a}$ and $GM \rightarrow 1$.

The equations of motion in dimensionless form are equivalent to the dynamical system

$$\begin{aligned} \frac{dz}{dT} &= \left(\gamma^2 - 1 + \frac{2z}{z^2 + \hat{a}^2} \right)^{1/2}, \\ \frac{dZ}{dT} &= V, \\ \frac{dV}{dT} &= \hat{\alpha} \frac{(1 - V^2)^{5/2}}{(1 - wV)^2} (w - V) + \frac{2z(z^2 - 3\hat{a}^2)}{(z^2 + \hat{a}^2)^3} (1 - 2V^2)Z, \end{aligned} \quad (39)$$

where we assume that $\gamma \geq 1$.

We have proved the following result: If $\hat{\alpha} > 0$, $0 \leq w < 1$, $z(0) > \sqrt{3}\hat{a}$, and

$0 < V(0) < 1$, then $\lim_{T \rightarrow \infty} V(T) = w$. That is, as time increases the clump speed approaches the drift speed of the ambient medium.

Equation (35) and the system (39) show how the tidal equation can in principle be generalized to include nongravitational forces. On the other hand, it is necessary to emphasize the qualitative significance of equation (35), since its gravitational part is valid only within a distance \mathcal{R} of the fiducial particle and its electromagnetic part is based on a rather simple model. If the tidal part is completely ignored, then the Lorentz force would lead to a monotonic deceleration of an initially ultrarelativistic clump toward w . Numerical experiments based on the system (39) demonstrate that the tidal part initially dominates, causing a very rapid drop in Γ toward $\sqrt{2}$, and this occurs mostly within the domain of validity of the tidal term, but then the electromagnetic term takes over and Γ slowly tends toward $(1 - w^2)^{-1/2}$. Figure 4 depicts a profile for the graph of Γ versus time, where the parameter values and initial conditions are chosen to be typical for a microquasar with $M = 10M_\odot$. According to our model (39) with electrical drift speed corresponding to $\Gamma = 2$ and with Lorentz acceleration coefficient $\hat{\alpha} = 10^{-7}$, an initial Lorentz factor of $\Gamma = 5$ decreases to $\Gamma \approx 1.5$ in about 0.25 sec and then very slowly increases to within 1% of $\Gamma = 2$ after 48 hours. More generally, for $\hat{\alpha} < 10^{-2}$ the timescale for the initial rapid decrease in Γ is about 0.1 sec. The corresponding total relaxation time to $\Gamma = 2$ is approximately $(50\hat{\alpha})^{-1}$ sec, so that for $\hat{\alpha}$ ranging from 10^{-3} to 10^{-11} , it ranges from 20 seconds to 64 years. For a quasar with $M = 10^8 M_\odot$, the timescale for the initial rapid decrease in Γ would be about two weeks.

To see that our result holds in general, let us note that $dz/dT > 0$ for $T > 0$. Thus, z is an increasing function of T , which is defined for $0 \leq T < \infty$. By viewing z as a new “time” in the dynamical system (39), it suffices to consider the system

$$\begin{aligned} \frac{dZ}{dz} &= \frac{1}{R(z)}V, \\ \frac{dV}{dz} &= \frac{1}{R(z)} \left(\hat{\alpha} \frac{(1 - V^2)^{5/2}}{(1 - wV)^2} (w - V) + \frac{2z(z^2 - 3\hat{\alpha}^2)}{(z^2 + \hat{\alpha}^2)^3} (1 - 2V^2)Z \right), \end{aligned} \quad (40)$$

where

$$R(z) := \left(\gamma^2 - 1 + \frac{2z}{z^2 + \hat{\alpha}^2} \right)^{1/2}.$$

In this system $dZ/dz > 0$. Hence, as before, it suffices to consider the scalar differential equation

$$\frac{dV}{dZ} = \hat{\alpha} \frac{(1 - V^2)^{5/2}}{(1 - wV)^2 V} (w - V) + 2Z \frac{S(Z)(S(Z)^2 - 3\hat{\alpha}^2)(1 - 2V^2)}{(S(Z)^2 + \hat{\alpha}^2)^3 V}, \quad (41)$$

where S is the function such that $S(Z(z)) = z$.

Direction fields of dV/dZ in the (Z, V) -plane are depicted in Figure 5 for the two cases $w > 1/\sqrt{2}$ and $w < 1/\sqrt{2}$. Graphs of typical solutions are also drawn. Since V stays bounded and the curvature $k(T)$ approaches zero very fast, it can

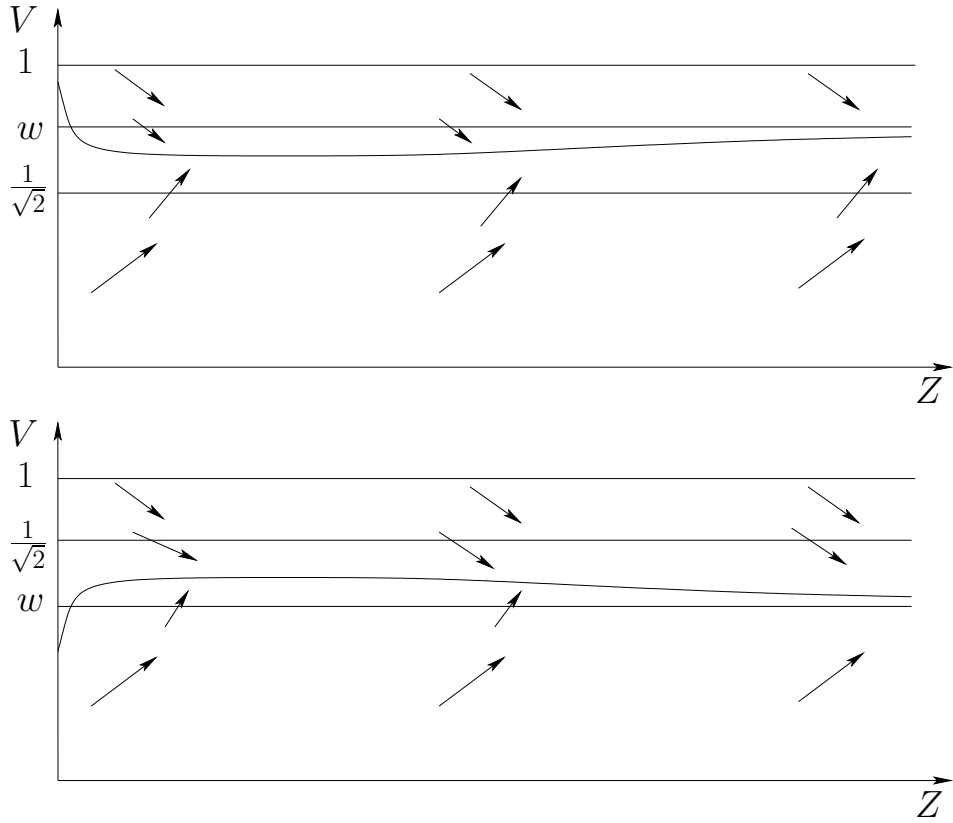


Figure 5: Schematic representation of direction fields and trajectories for the dynamical system (41).

be shown that the second term on the right-hand side of equation (41) rapidly approaches zero as $T \rightarrow \infty$. Also, with this term set to zero, the dynamical system (41) has an asymptotically stable steady state at $V = w$. For large Z , the first term is dominant; therefore, the limiting value of the solution is w .

6 Discussion

This paper is devoted to a simple model of the evolution of the speed of a clump in a relativistic flow once it emerges from the environment immediately surrounding the central source. Combined with a realistic treatment of plasma effects, our theoretical approach should be of interest in the study of astrophysical jets. If the motion of the clump is force-free, then it follows from the repeated application of the generalized Jacobi equation that the clump speed tends to $V_T = 1/\sqrt{2}$ corresponding to $\Gamma = \sqrt{2}$. On the other hand, if the force-

free condition is not satisfied, the clump speed tends to $V_L = w$, where w is the electrical drift speed. In fact, if the tidal component initially dominates, as would be the case for most microquasars, then starting with an initial speed almost equal to unity, the tidal force is responsible for the initial rapid decrease of the velocity toward $1/\sqrt{2}$, but then the Lorentz term takes over and the velocity slowly approaches w . On the other hand, if the Lorentz term is dominant, as would be the case for most quasars, there is in effect a relatively slow decrease of the velocity toward w .

References

- [1] P. Padovani and C. M. Urry, *Astrophys. J.* **387**, 449 (1992).
- [2] R. C. Vermeulen and M. H. Cohen, *Astrophys. J.* **430**, 467 (1994).
- [3] R. Fender, *Lect. Notes Phys.* **589**, 101 (2002), [astro-ph/0109502].
- [4] R. Fender, in Compact Stellar X-ray Sources, eds. W.H.G. Lewin and M. van der Klis (Cambridge, Cambridge University Press, 2004), [astro-ph/0303339].
- [5] D. Burgarella, M. Livio and C. P. O’Dea, eds., Astrophysical Jets (Cambridge, Cambridge University Press, 1994).
- [6] A. W. Guthmann, M. Georganopoulos, A. Marcowith and K. Manolaku, eds., Relativistic Flows in Astrophysics, *Lect. Notes Phys.* **589** (Berlin, Springer, 2002).
- [7] J. L. Synge, Relativity: The General Theory (Amsterdam, North-Holland, 1960).
- [8] C. Chicone and B. Mashhoon, *Class. Quantum Grav.* **19**, 4231 (2002).
- [9] H. Quevedo and B. Mashhoon, *Phys. Rev. D* **43**, 3902 (1991).
- [10] B. Mashhoon and J.C. McClune, *Mon. Not. R. Astron. Soc.* **262**, 881 (1993).
- [11] J.K. Beem, P.E. Ehrlich and K.L. Easley, Global Lorentzian Geometry, 2nd ed. (New York, Dekker, 1996) ch. 2.
- [12] J. Contopoulos, *Astrophys. J.* **446**, 67 (1995).
- [13] L. Spitzer Jr., Physics of Fully Ionized Gases, 2nd rev. ed. (New York, Interscience, 1962).
- [14] B. Punsly, Black Hole Gravitohydrodynamics (New York, Springer-Verlag, 2001).